

## Extreme $\alpha$ -clustering in the $^{18}\text{O}$ nucleus

E.D. Johnson<sup>1,a</sup>, G.V. Rogachev<sup>1</sup>, V.Z. Goldberg<sup>2</sup>, S. Brown<sup>1,3</sup>, D. Robson<sup>1</sup>, A.M. Crisp<sup>1</sup>, P.D. Cottle<sup>1</sup>, C. Fu<sup>2</sup>, J. Giles<sup>1</sup>, B.W. Green<sup>1</sup>, K.W. Kemper<sup>1</sup>, K. Lee<sup>1</sup>, B.T. Roeder<sup>1,2</sup>, and R.E. Tribble<sup>2</sup>

<sup>1</sup> Department of Physics, Florida State University, Tallahassee, FL 32306, USA

<sup>2</sup> Cyclotron Institute, Texas A&M University, College Station, TX 77843, USA

<sup>3</sup> The University of Surrey, Guildford, Surrey, UK

Received: 19 June 2009 / Revised: 24 August 2009

Published online: 22 October 2009 – © Società Italiana di Fisica / Springer-Verlag 2009

Communicated by B.R. Fulton

**Abstract.** The structure of the  $^{18}\text{O}$  nucleus at excitation energies above the  $\alpha$  decay threshold was studied using  $^{14}\text{C} + \alpha$  resonance elastic scattering. A number of states with large  $\alpha$  reduced widths have been observed, indicating that the  $\alpha$ -cluster degree of freedom plays an important role in this  $N \neq Z$  nucleus. A  $0^+$  state with an  $\alpha$  reduced width exceeding the single-particle limit was identified at an excitation energy of  $9.9 \pm 0.3$  MeV. We discuss evidence that states of this kind are common in light nuclei and give possible explanations of this feature.

**PACS.** 21.10.Gv Nucleon distributions and halo features – 24.30.-v Resonance reactions – 25.55.Ci Elastic and inelastic scattering

After the discovery of the neutron it was understood that  $\alpha$ -particles cannot exist in the bulk of a nucleus at normal nuclear density due to the need for antisymmetrization over all nucleons. Still,  $\alpha$ -clustering manifests itself in light  $4N$  nuclei such as  $^8\text{Be}$ ,  $^{12}\text{C}$ ,  $^{16}\text{O}$ , and  $^{20}\text{Ne}$  through the existence of twin quasi-rotational bands of states with alternating parities and  $\alpha$ -particle reduced widths which are close to the single-particle limit (see the recent review by M. Freer [1] and references therein).

There are different approaches that attempt to describe the shell model and the  $\alpha$ -cluster structure of nuclei on an equal footing in order to shed light on the interplay between the  $\alpha$ -cluster and single-particle degrees of freedom [1]. Data on the nucleon decay of  $\alpha$ -cluster states would be instrumental for such efforts. However, this data is practically absent due to the much higher nucleon decay thresholds in comparison with the thresholds for the  $\alpha$  decay in the  $4N$  nuclei. It is more promising to observe the nucleon decay from the  $\alpha$ -cluster states in  $N \neq Z$  nuclei where the nucleon and  $\alpha$ -particle thresholds are close to each other. The study of non-self-conjugate nuclei has an advantage in that one can investigate  $\alpha$ -cluster states in mirror systems and use the Coulomb shift to extract information on the relationship between the cluster and single-particle degrees of freedom. Unfortunately, the data on the  $\alpha$ -cluster structure of  $N \neq Z$  nuclei are generally very limited.

The current interest in the  $\alpha$ -particle interaction with  $N \neq Z$  nuclei is also strongly motivated by astrophysics [2]. Even if astrophysical reactions involving helium do not proceed through the strong  $\alpha$ -cluster states (because of high excitation energy), these states can provide  $\alpha$  width to the states that are closer to the region of astrophysical interest through configuration mixing [3]. However, the study is complicated by experimental difficulties and the need for multi-channel analysis of many broad overlapping, interfering resonances. This is illustrated by the previous investigations of the  $\alpha + ^{14}\text{C}$  interaction. In the first [4] (and only) study of the resonances in the  $\alpha + ^{14}\text{C}$  elastic scattering, the experimental difficulties were minimized by using a solid (radioactive)  $^{14}\text{C}$  target. However, only a few assignments for some strong and sharp resonances were made. Goldberg *et al.* [5] reanalyzed the data of [4] using a simplified version of the  $\mathbf{R}$ -matrix theory. In the analysis approach used in [5] only the elastic scattering channel was considered explicitly, while the influence of all other decay channels was parametrized through a  $\Gamma_\alpha/\Gamma_{tot}$  parameter for each resonance. They gave a few new assignments, but again many of them were tentative. The need for a more detailed investigation, better fit and new experimental data was pointed out in [5]. The  $\beta$ -delayed  $\alpha$  spectrum of  $^{18}\text{N}$  was measured in refs. [6, 7]. Due to the high selectivity of  $\beta$  decay only  $1^-$  states were observed in the  $^{18}\text{O}$  spectrum. Several broad  $1^-$  states were identified in [7]. In this letter we report new measurements of  $\alpha + ^{14}\text{C}$  resonance elastic scattering

<sup>a</sup> e-mail: edj04@fsu.edu

made using the Thick Target Inverse Kinematics (TTIK) method [8]. This experimental approach provided good statistics and excitation functions which were remarkably free of any background. The data provided a basis for a successful analysis of the excitation functions using a complete multi-level, multi-channel **R**-matrix approach [9]. As a result, we found that in  $^{18}\text{O}$  there is a system of strong  $\alpha$ -cluster states. Both  $\alpha$  and nucleon reduced widths of these  $\alpha$ -cluster states were determined from the multi-channel **R**-matrix fit. The main focus of our discussion in this letter is the surprising finding of a state with an  $\alpha$ -particle width exceeding the single-particle limit. We interpret this as evidence for extreme  $\alpha$ -clustering and argue that existing experimental data on light 4N nuclei indicates that this is a common feature for nuclei in this mass range.

The experiment was carried out at the Florida State University John D. Fox Superconducting Accelerator Laboratory. The 25 MeV  $^{14}\text{C}$  beam was produced by an FN Tandem Van-de-Graff accelerator and directed into the scattering chamber, which consisted of two compartments. The first compartment was under vacuum, the second was filled with 99.9% pure helium gas ( $^4\text{He}$ ). The two compartments were separated with a  $1.27\ \mu\text{m}$  Havar foil. The intensity and quality (focusing and alignment) of the beam was monitored using elastic scattering off a gold target, placed in the middle of the vacuum compartment, and from the Havar foil (the energy of the beam is less than the C + Co Coulomb barrier). The helium gas pressure in the second compartment was adjusted to stop the incoming beam before an array of silicon detectors located at a distance of  $\sim 40\text{ cm}$  from the Havar foil. Details of the method are given in [10].

The excitation functions for the  $^{14}\text{C} + \alpha$  elastic scattering covering the center-of-mass (c.m.) energy region of 2.0–4.5 MeV were measured at 20 different angles. The observed background was less than 1%. Conversion of the laboratory excitation functions into the c.m. was made on a bin-by-bin basis using a computer code which takes into account the relevant experimental conditions [11]. The accuracy of the absolute normalization of the cross-section, performed by the monitor detector using the elastic scattering of the  $^{14}\text{C}$  beam off the Havar foil, is 15%. The uncertainty in the specific energy loss of  $^{14}\text{C}$  in helium is responsible for a 20 keV uncertainty in the absolute calibration of the c.m. energy.

The analysis of the excitation functions was performed using a multi-level, multi-channel **R**-matrix approach [9]. The  $^{14}\text{C} + \alpha$  excitation functions measured in this experiment are continuous, which excludes the possibility of missing a narrow resonance. The sensitivity of the data is demonstrated by the fact that even the  $2^+$  state at 8.213 MeV (1.986 MeV c.m.), which has width of  $\sim 1\text{ keV}$ , is still clearly visible in the  $180^\circ$  excitation function (see the inset in fig. 1). In addition, data from previous measurements of the  $^{14}\text{C}(\alpha, \alpha)$  [4] and  $^{14}\text{C}(\alpha, n)$  [12] excitation functions were used. The overall fit was very good with  $\chi^2/\nu = 1.64$  for the c.m. energy range 2.65–4.45 MeV. The **R**-matrix fit to the  $^{14}\text{C}(\alpha, \alpha)$  data is shown in fig. 1.

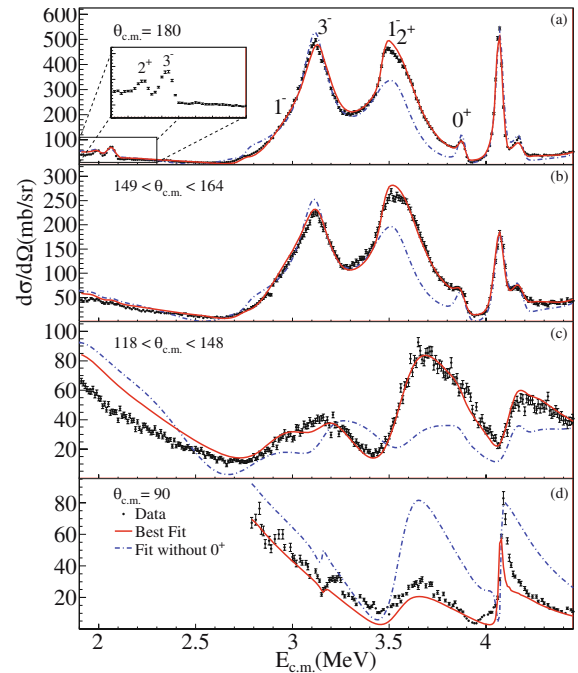


**Fig. 1.** (Color online) The excitation functions for  $\alpha + ^{14}\text{C}$  elastic scattering measured at various angles, demonstrating the influence of the broad  $J^\pi = 0^+$  state reported here. The top three panels are data from the present experiment, while the bottom panel at  $90^\circ$  is taken from [4]. The experimental technique used here yields a continuously varying scattering angle for each excitation function except at  $180^\circ$ ; hence, the angular ranges shown in the middle two panels overlap. The red solid curves show the best **R**-matrix fit with the broad  $J^\pi = 0^+$  state at a resonance energy of 3.7 MeV (corresponding to an excitation energy of 9.9 MeV in  $^{18}\text{O}$ ), while the blue dash-dotted curve is the best fit without this state. States with large  $\alpha$  reduced width are labeled.

As can be expected most of the states also have substantial neutron widths, which are obtained through the  $(\alpha, \alpha)$  fit. We verified that the  $^{14}\text{C}(\alpha, n)$  total cross-section from ref. [12] is reproduced rather well by **R**-matrix calculations performed using the parameters from the  $^{14}\text{C}(\alpha, \alpha)$  fit. One can notice that the **R**-matrix fit underestimates the experimental cross-section at the lowest energies for angles far from  $180^\circ$ . This is understood to be an effect of the finite dimensions of the beam spot.

The fourth panel in fig. 1 is  $90^\circ$  data from [4]. The spectrum at  $90^\circ$  in c.m. is only influenced by states with even angular momentum and positive parity. This is an important simplification and makes the spectrum at  $90^\circ$  very valuable for the **R**-matrix analysis. Clearly, our data contains this information. However, for the purpose of a more clear representation of the data we used the spectrum of [4] at  $90^\circ$  rather than construct the  $90^\circ$  spectrum from several different detectors.

Twenty-four resonances were used to fit the data, some of them were previously known. Detailed discussion of the analysis procedure and notes on the properties of each state will be given in a follow-up paper. Levels with large  $\alpha$ -cluster reduced widths ( $\theta_\alpha^2 > 0.1$ ) are given in table 1.

**Table 1.** Levels with large  $\alpha$  reduced width in  $^{18}\text{O}$ .  $\Gamma_{tot}$ ,  $\Gamma_\alpha$  and  $\Gamma_n$  are the total and partial  $\alpha$  and neutron widths, respectively.  $\theta_\alpha^2 = \gamma_\alpha^2/\gamma_{SP}^2$  is the dimensionless reduced width for the  $\alpha$  channel, where  $\gamma_{SP}^2 = \hbar^2/\mu R^2$  is the single-particle limit, calculated at channel radius 5.2 fm. Error bars are dominated by systematic errors in absolute energy calibration and absolute cross-section normalization.

$E_{exc}$ (MeV)	$J^\pi$	$\Gamma_{tot}$ (keV)	$\Gamma_\alpha$ (keV)	$\theta_\alpha^2$	$\Gamma_n$ (keV)
9.17(3)	$1^-$	229(50)	200(50)	0.24	29(7)
9.39(3)	$3^-$	151(50)	100(48)	0.45	51(15)
9.75(4)	$1^-$	628(100)	585(100)	0.43	43(10)
9.77(3)	$2^+$	251(50)	172(45)	0.20	79(20)
9.9(3) <sup>a</sup>	$0^+$	2100(500) <sup>b</sup>	2100(500)	2.6	N/S <sup>c</sup>

<sup>a</sup> The excitation energy of the  $0^+$  state is defined as maximum of the  $\sin^2 \delta_\alpha$ , where  $\delta_\alpha$  is the  $\ell = 0$  phase shift (see fig. 2).

<sup>b</sup> The width of the  $0^+$  state is defined as FWHM of the  $\sin^2 \delta_\alpha$ .

<sup>c</sup> The **R**-matrix fit is not sensitive to the neutron partial width of the  $0^+$  state within reasonable limits.

Five levels with dimensionless  $\alpha$  reduced width greater than 0.1 have been observed in  $^{18}\text{O}$  in the narrow excitation energy range between 9.1 and 9.9 MeV. Three of them have been suggested in previous publications [6, 5, 7]. The strong  $\alpha$ -cluster state at  $9.0 \pm 0.2$  MeV was first suggested in [6], where the  $1^-$  spin parity assignment was made on the basis of the population of this state in  $^{18}\text{N}$   $\beta$  decay. A more recent  $^{18}\text{N}$   $\beta$  decay experiment [7] confirmed the  $1^-$  state at 9.16 MeV with a width of  $\Gamma = 420 \pm 200$  keV. Our **R**-matrix fit requires a  $1^-$  state at an excitation energy of  $9.17 \pm 0.03$  MeV in good agreement with [7]. The width of this state is lower in the present work ( $230 \pm 50$  keV) but still within the error bars of [7]. Another  $1^-$  state observed at  $9.85 \pm 0.5$  MeV in [7] with a width of  $560 \pm 200$  keV is in very good agreement with the results of this work. The  $3^-$  at 9.39 MeV was previously suggested in [5] and has excellent agreement with the present results. The strong  $\alpha$ -cluster  $2^+$  state at 9.77 MeV is identified for the first time in this work.

The most surprising finding of this work was the observation of a very broad  $0^+$  state at  $9.90 \pm 0.3$  MeV. Generally, it is not easy to identify very broad resonances because they are disguised by interference with the sharp ones. This is especially true for the  $0^+$  resonances. Nevertheless, the existence of the broad  $\alpha$ -cluster  $0^+$  state in the spectrum of  $^{18}\text{O}$  is certain. The effect of this state on the cross-section is demonstrated in fig. 2. The cross-section is lowered dramatically due to the destructive interference of the  $0^+$  state with Coulomb scattering. The Rutherford cross-section and the Rutherford with the broad  $0^+$  state at 9.90 MeV (3.7 MeV c.m.) are shown at two c.m. angles,  $90^\circ$  and  $180^\circ$ , in fig. 2. Without this destructive interference it is not possible to reproduce the experimental data. As seen in the bottom panel of fig. 1, the cross-section calculated without the broad  $0^+$  state is significantly larger than the experimental one. This is a clear indication of a  $0^+$  resonance. All other resonances would not

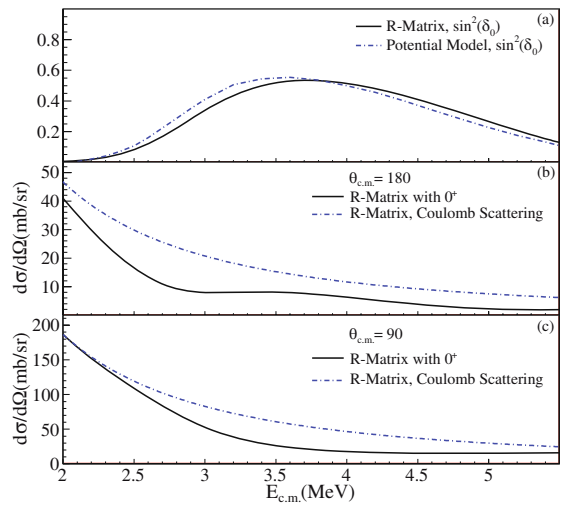


**Fig. 2.** (Color online) The top panel is the  $\sin^2 \delta_{\ell=0}$  from the **R**-matrix fit (solid curve) compared to the potential model prediction (dash-dotted curve). The middle and the bottom panel demonstrate influence of the broad  $0^+$  state on the cross-section at  $180^\circ$  and  $90^\circ$  c.m., respectively. The dash-dotted curve corresponds to the Coulomb scattering cross-section and the solid curve shows the differential cross-section from the interference of the broad  $0^+$  with Coulomb scattering.

produce the right interference with the Rutherford scattering and could not be broad enough. One can follow the effect of the  $0^+$  level at different angles in fig. 1 and reach the same conclusion. We also considered the possibility of two narrower  $0^+$  states instead of one. The decisive factor against it was that the characteristic interference pattern between two nearby  $0^+$  states was not observed experimentally. The  $\alpha$ -particle reduced width amplitudes of the  $0^+$  state with channel radii of 5.2 and 6.5 fm are 1.38 and 0.66  $\text{MeV}^{1/2}$ , respectively. Formally, both values exceed the single-particle limit. Using a classical approach one can interpret this as evidence that the  $\alpha$ -particle resides at a large distance from the  $^{14}\text{C}$  core.

A more detailed description of the observed  $0^+$  state in  $^{18}\text{O}$  can be given using the potential model approach. The parameters of this model were extracted starting from the potential model for  $^8\text{Be}$  given in [13], which provides an accurate description of the  $s$ -wave  $\alpha$ - $\alpha$  phase shift over a large energy range. First, this potential model was used to investigate the  $^{16}\text{O} + \alpha$  interaction by assuming the  $\alpha$ -cluster model [14] for the ground state of  $^{16}\text{O}$ , properly modified [15] to include antisymmetry and the strong repulsion between nucleons. The strong interaction between the incoming  $\alpha$  and the target “alphas” is obtained by folding the Buck interaction [13] with the target  $\alpha$ -density in the ground state and produces a nuclear potential with several Pauli forbidden states. These are removed by adding a repulsive Gaussian potential in the relative  $\alpha$ - $^{16}\text{O}$  radial coordinate. The result is to produce a bound state for the ground state of  $^{20}\text{Ne}$  and a broad  $0^+$  state at 4 MeV in c.m. as observed in [16] with the same  $0^+$  phase shift behavior. The corresponding density dis-

tribution for this  $0^+$  resonance has an inner peak at 2 fm and an outer peak at 5 fm. The outer peak is at a separation distance beyond the sum of the charge radii of  $^4\text{He}$  and  $^{16}\text{O}$  and it contains most of the probability indicating that the broad  $0^+$  resonance in  $^{20}\text{Ne}$  appears to be a state with extreme  $\alpha$ -clustering.

The  $^{18}\text{O}$  system was then investigated using the  $^{20}\text{Ne}$  potential as a starting point but small changes in the strengths of the folded and repulsive potentials were used to reproduce the ground state of  $^{18}\text{O}$ . This potential produces a broad  $0^+$  state at 3.5 MeV in c.m. The experimental  $s$ -wave resonance phase shift from the  $\mathbf{R}$ -matrix fit (solid black curve in fig. 2a) is reproduced rather well by such a potential (dash-dotted blue curve in fig. 2a). The density distribution for the broad  $0^+$  state in  $^{18}\text{O}$  is similar to the one in  $^{20}\text{Ne}$ . The outer peak is at 5.5 fm which is considerably larger than the sum of the charge radii for  $^4\text{He}$  and  $^{14}\text{C}$  and even larger than the  $^{20}\text{Ne}$  outer peak radius. This latter result is presumably due to the larger Coulomb barrier in the  $^{20}\text{Ne}$  system. Both systems appear to show well-separated  $\alpha$ -cluster configurations that correspond to extreme  $\alpha$ -clustering.

Due to the large distance between the  $\alpha$ -cluster and the core, one can speculate that levels of this kind should be a general feature of the interaction between an  $\alpha$ -particle and a core nucleus which is independent of the specific structure of the core. If this is the case then resonances of this kind should be present in all nearby nuclei at excitation energies on the order of a few MeV above the  $\alpha$  decay threshold. Indeed, a broad (3 MeV)  $0^+$  level at an excitation energy of 10.3 MeV ( $\sim 3$  MeV above the  $\alpha$  threshold) appears in  $^{12}\text{C}$  [17]. Recently, the parameters of this  $0^+$  level were revised in measurements of the  $3\alpha$  decay of this level populated after  $\beta$  decay of  $^{12}\text{B}$  or  $^{12}\text{N}$  [18,19]. The new parameters, as given in [19], are an excitation energy of 10.73 MeV and a width of 1.72 MeV. However, there are still significant uncertainties in these values.

There is much more controversy related to a possible broad  $0^+$  level in  $^{16}\text{O}$  at  $\sim 11.3$  MeV excitation energy ( $\sim 4$  MeV above the threshold) [20], since there are conflicting results for this state [21–25]. However, the most recent article presented clear evidence for broad  $0^+$  strength at the excitation energy in question [26,27]. Finally, a broad  $0^+$  level ( $\Gamma > 800$  keV) at  $\sim 4$  MeV above the  $\alpha$  decay threshold was observed in  $^{20}\text{Ne}$  [16]. This result has not been questioned since it was first reported.

One may refer to these states as “ $\alpha$ -halo” states. This term was first suggested in [28] and has merit. Also, one should not link directly unbound  $\alpha$ -halo resonances with bound neutron halo configurations found in some weakly bound neutron-rich nuclei.

While the purely single- $\alpha$ -particle nature of these states is clear it is interesting to consider the possible quantum-mechanical reasons behind the emergence of such pure configurations. The answer may be a “super-radiance” phenomenon (see for example [29]). Super-radiance emerges in the limit of strong coupling to the continuum (broad strongly overlapping resonances of the same spin parity) and represents the accumulation of the

total summed  $\alpha$  width from the unperturbed intrinsic states by one very broad (super-radiant) resonance. Since the centrifugal barrier is absent for  $\ell = 0$  states the condition of strong continuum coupling is more likely realized for the  $0^+$  states than for the states of any other spin parity.

In summary, we are only in the beginning phases of studying the  $\alpha$ -cluster structure of light  $N \neq Z$  nuclei. Here we report a measurement of the  $^{14}\text{C} + \alpha$  elastic scattering excitation functions including a successful analysis using the complete  $\mathbf{R}$ -matrix framework. We identified that the  $\alpha$ -cluster states in  $^{18}\text{O}$  have many surprising properties, the foremost of which is the discovery of a broad,  $\ell = 0$  state which we suggest may be present in other nuclei in this mass range. This conclusion is strengthened through comparison with previous results [16–20,26]. There is much work still ahead to prove this point. The discovery of the broad states in question within odd-even nuclei is an especially important and difficult task. Nevertheless, the possible influence that these broad low spin resonances may have on astrophysically important reaction rates along with the insight they can give into  $\alpha$ -clustering justifies these efforts.

The authors are grateful to Prof. A. Volya for useful comments and discussions. This work was supported by the NSF under grant number PHY-456463 and the DOE under grant number DE-FG02-93ER40773.

## References

1. M. Freer, Rep. Prog. Phys. **70**, 2149 (2007).
2. A. Aprahamian, K. Langanke, M. Wiescher, Prog. Part. Nucl. Phys. **54**, 535 (2005).
3. C. Fu, V. Goldberg, G. Rogachev *et al.*, Phys. Rev. C **77**, 064314 (2008).
4. G. Morgan *et al.*, Nuc. Phys. A **148**, 480 (1970).
5. V.Z. Goldberg *et al.*, Phys. At. Nucl. **68**, 1123 (2004).
6. Z. Zhao *et al.*, Phys. Rev. C **39**, 1985 (1989).
7. L. Buchmann *et al.*, Phys. Rev. C **75**, 012804(R) (2007).
8. K.P. Artemov *et al.*, Sov. J. Nucl. Phys. **52**, 408 (1990).
9. A. Lane, R. Thomas, Rev. Mod. Phys. **30**, 257 (1958).
10. E. Johnson, PhD Thesis, Florida State University (2008).
11. G. Rogachev, PhD Thesis, Kurchatov Institute (1999).
12. J.K. Bair *et al.*, Phys. Rev. **144**, 799 (1966).
13. B. Buck, in *International Conference on Clustering Aspects of Nuclear Structure and Nuclear Reactions* (D. Reidel Publishing Company, Dordrecht, Holland, 1984) p. 71.
14. J. Wheeler, Phys. Rev. **52**, 1083 (1937).
15. D. Robson, Phys. Rev. Lett. **42**, 876 (1979).
16. L. McDermott *et al.*, Phys. Rev. **118**, 175 (1960).
17. D. Tilley *et al.*, Nucl. Phys. A **636**, 247 (1998).
18. H.O.U. Fynbo *et al.*, Nature **433**, 136 (2005) <http://dx.doi.org/10.1038/nature03219>.
19. C. Diget *et al.*, Nucl. Phys. A **760**, 3 (2005).
20. F. Ajzenberg-Selove, Nucl. Phys. A **490**, 1 (1988).
21. J. Bittner, R. Moffat, Phys. Rev. **96**, 374 (1954).
22. W. Bohne, Nucl. Phys. A **128**, 537 (1969).
23. H. Fulbright, Phys. Rev. **184**, 1068 (1969).

24. G. Clark, D. Sullivan, P. Treacy, Nucl. Phys. A **110**, 481 (1968).
25. D. Tilley, H. Weller, C. Cheves, Nucl. Phys. A **564**, 1 (1993).
26. Y.W. Lui, H. Clark, D. Youngblood, Phys. Rev. C **64**, 064308 (2001).
27. Y.W. Lui, private communications.
28. Y. Funaki, A. Tohsaki, H. Horiuchi, P. Schuck, G. Ropke, Eur. Phys. J. A **24**, 321 (2005).
29. A. Volya, V. Zelevinsky, J. Opt. B: Quantum Semiclass. Opt. **5**, S450 (2003).